Modeling the Effects of Napping and Non-napping Patterns of Light Exposure on the Human Circadian Oscillator

Running title: Modeling Napping Effects on the Human Circadian Oscillator

Shelby R. Stowe[1], Monique K. LeBourgeois[2], & Cecilia Diniz Behn[1,3]

[1] Department of Applied Mathematics and Statistics, Colorado School of Mines, Golden, CO, USA

[2] Department of Integrative Physiology, University of Colorado Boulder, Boulder, CO, USA

[3] Division of Endocrinology, Department of Pediatrics, University of Colorado Denver Anschutz Medical Campus, Aurora, CO, USA

Corresponding author:

Cecilia Diniz Behn

Mailing address: Colorado School of Mines, Department of Applied Mathematics and Statistics, 1500 Illinois Street, Golden CO 80401

Phone: 303-273-3872

Fax: 303-273-3875

Email: cdinizbe@mines.edu

Abstract

In early childhood, consolidation of sleep from a biphasic to a monophasic sleep-wake pattern, i.e., the transition from sleeping during an afternoon nap and at night to sleeping only during the night, represents a major developmental milestone. Reduced napping behavior is associated with an advance in the timing of the circadian system; however, it is unknown if this advance represents a standard response of the circadian clock to altered patterns of light exposure or if it additionally reflects features of the developing circadian system. Using a mathematical model of the human circadian pacemaker, we investigated the impact of napping and non-napping patterns of light exposure on entrained circadian phases. Simulated light schedules were based on published data from 20 children (34.2±2.0 months) with habitual napping or non-napping sleep patterns (15 nappers). We found the model predicted different circadian phases for napping and non-napping light patterns: both the decrease in afternoon light during the nap and the increase in evening light associated with napping toddlers' later bedtimes contributed to the observed circadian phase difference produced between napping and non-napping light schedules. We systematically quantified the effects on phase shifting of nap duration, timing, and light intensity, finding larger phase delays occurred for longer and earlier naps. Additionally, we simulated phase response curves to a 1 h light pulse and 1 h dark pulse to predict phase- and intensity-dependence of these changes in light exposure. We found the light pulse produced larger shifts compared to the dark pulse, and we analyzed the model dynamics to identify the features contributing to this asymmetry. These findings suggest that napping status affects circadian timing due to altered patterns of light exposure, with the dynamics of

the circadian clock and light processing mediating the effects of the dark pulse associated with a daytime nap.

Keywords: mathematical model, circadian oscillator, phase response curve, napping, early childhood, light

Introduction

The approximately 24-h cycles known as circadian rhythms represent a physiological feature of nearly all living organisms and are observed in humans as early as 9 to 12 weeks of age (Kennaway et al., 1992; Kennaway et al., 1996). Circadian rhythms are produced by an intra-cellular molecular clock that is mediated through genetic feedback loops (Hardin et al., 1990; Welsh et al., 1995; Price et al., 1998; Dunlap, 1999; Gachon et al., 2004; Oster, 2006). The circadian system requires external time cues, known as zeitgebers, to maintain alignment with the 24-h solar day. Many aspects of daily life act as zeitgebers, but the primary stimulus to the circadian system is the 24-h light:dark cycle (Czeisler et al., 1981; Roenneberg and Foster, 1997; Duffy and Wright, 2005). Light affects the circadian system through photoreceptors, cells in the retina that are responsive to light (Foster et al., 1991; Provencio et al., 2000; Hattar et al., 2002). Light exposure causes intrinsically photosensitive retinal ganglion cells (ipRGCs) to fire action potentials (Berson et al., 2002), sending signals to the hypothalamus via the retinohypothalamic tract (Moore et al., 1995). These signals are received by cells in the master clock of the circadian system, the suprachiasmatic nuclei (SCN) (Moore and Eichler, 1972; Stephan and Zucker, 1972; Ralph et al., 1990; Welsh et al., 2010), and entrain the SCN to the 24-h day (Czeisler et al., 1999; Duffy and Wright, 2005). Signaling from the SCN coordinates other circadian rhythms in the body, thus enabling the circadian system to align with its environment (Yamazaki et al., 2000; Dibner et al., 2010; Mohawk et al., 2012).

Light exposure is gated by sleep-wake patterns, which change across the lifespan (Iglowstein et al., 2003; Crowley et al., 2014; Duffy et al., 2015). In early childhood, the consolidation of sleep into a single nighttime episode is a major developmental milestone, and changes in sleep timing, duration, and circadian phase occur with this transition (Iglowstein et al., 2003; Crosby, 2005; Jenni and LeBourgeois, 2006; Akacem et al., 2015). Longitudinal data indicate a decrease in total 24-h sleep duration from an average of 13 h at 2 years to 11 h at 6 years of age (Iglowstein et al., 2003). This decrease in total sleep time is primarily attributed to the transition from a biphasic to monophasic sleep-wake pattern, with napping frequency and duration gradually declining with age (Crosby, 2005; Jenni and LeBourgeois, 2006). The change in the timing of sleep may be associated with altered patterns of light exposure. In preschool-aged children, decreased napping frequency may increase light exposure in the afternoon, earlier bedtime may decrease light exposure in the evening, and decreased total time in bed may increase daily light exposure (Iglowstein et al., 2003; Crosby, 2005; Jenni and LeBourgeois, 2006; Dumont and Beaulieu, 2007; Akacem et al., 2015). In addition to changes in patterns of light exposure that are associated with increasing age, eye physiology and light sensitivity of the circadian clock may also experience nonlinear changes across the lifespan (Turner and Mainster, 2008; Higuchi et al., 2014).

Experimental work has determined that the phase of the human circadian clock is affected by photoperiod (Sumová et al., 2004; Meijer et al., 2007; Coomans et al., 2015) as well as the timing, duration, and intensity of acute light exposure (Honma and

Honma, 1988; Czeisler et al., 1989; Zeitzer et al., 2000; Burgess and Eastman, 2004; Duffy and Wright, 2005; Wright et al., 2005). Phase response curves (PRCs) summarize the response of the circadian oscillator to a stimulus given at different circadian phases. PRCs to various light levels and durations have been established in adults (Honma and Honma, 1988; Czeisler et al., 1989; Minors et al., 1991; Jewett et al., 1994; Van Cauter et al., 1994; Khalsa et al., 2003; St Hilaire et al., 2012) and adolescents (Crowley and Eastman, 2017). These PRCs demonstrate that the sensitivity of the circadian system to light varies across the 24-h day, causing phase delays in the hours around bedtime (early in the subjective night) and phase advances in the hours around wake time (late in the subjective night and early in the subjective day). Similarly, data from experimental studies in rodents show that dark pulses produce phase shifts in opposite directions compared to light pulses, but both dark and light pulse PRCs show similar phase-dependence (Boulos and Rusak, 1982; Dwyer and Rosenwasser, 2000; Rosenwasser and Dwyer, 2002). However, in rodents, dark pulses also induce locomotor activity which can contribute to these effects (Dwyer and Rosenwasser, 2000; Rosenwasser and Dwyer, 2002). In humans, experimental data suggest that dark exposure in the morning can delay circadian phase and dark exposure in the evening can advance circadian phase, producing phase shifts opposite to those due to light exposure (Buxton et al., 2000).

The circadian system's response to light exposure across all circadian phases has yet to be determined in early childhood; however, recent findings from fundamental childhood circadian studies suggest that the central clock is highly sensitive to light exposure around bedtime (Higuchi et al., 2014; Akacem et al., 2016; Akacem et al., 2018; Hartstein et al., 2022a; Hartstein et al., 2022b). In preschool children, an approximately 40 min advance in circadian timing and earlier bedtime has been associated with decreased napping frequency (Akacem et al., 2015). However, it is unknown if this advance represents a standard response of the circadian clock to altered patterns of light exposure driven by changes in sleep need, or if it additionally reflects features of the developing circadian system. In this study, we use a mathematical model of the human circadian oscillator (Forger et al., 1999) to investigate the effects of napping and non-napping patterns of light exposure on circadian phase.

Mathematical modeling of human circadian rhythms is well established and includes models of the molecular clock (Forger and Peskin, 2003; Mirsky et al., 2009; Kim and Forger, 2012), phenomenological models based on sinusoids (Borbély, 1982; Daan et al., 1984) or modified van der Pol limit cycle oscillators (Kronauer et al., 1982; Forger et al., 1999; St Hilaire et al., 2007), and models reflecting SCN physiology (Abraham et al., 2010; Hannay et al., 2018; Hannay et al., 2019). Light plays a major role in some of these circadian models, with the modeled dynamics of light processing enabling the simulation of experimentally observed light responses (Forger et al., 1999; Kronauer et al., 1999). In addition, analysis of these models provides insight into circadian entrainment to light:dark cycles and responses to perturbations in light exposure (Forger et al., 1999; Skeldon et al., 2016; Diekman and Bose, 2018; Piltz et al., 2020; Stack et al., 2020; Diekman and Bose, 2022). Light input is often modeled with a direct forcing term, but additional dynamics reflecting the physiology of light processing may also be considered. In a modified van der Pol-type clock model, Kronauer and colleagues introduced an additional variable to account for putative photoreceptor dynamics (Kronauer et al., 1999). This approach enabled their model to respond appropriately to both extended (7 h) and brief (15 min) light stimuli while also incorporating intensity dependence, and these dynamics were incorporated into subsequent models (Forger et al., 1999; St Hilaire et al., 2007; Gleit et al., 2013; Hannay et al., 2019). We considered several circadian pacemaker models, and we focus on a van der Pol-type circadian clock model introduced by Forger and colleagues that includes these photoreceptor dynamics (Forger et al., 1999). This model has been fit to and validated on data from multiple experimental protocols with adult participants (Jewett et al., 1991; Khalsa et al., 1997; Forger et al., 1999; Stack et al., 2020), but it has not been tested in young children.

To analyze the effects of different patterns of light exposure on predicted circadian phase, we entrained the model to the light:dark schedules of napping and non-napping preschool children (Akacem et al., 2015) and investigated the effects of napping and later bedtimes on circadian phase. We also systematically studied the contributions of nap timing, duration, and light intensity on phase shifting of the circadian clock. We simulated a modified PRC protocol to a 1 h light and 1 h dark stimulus to quantify and compare the effects of light and dark pulses at different phases under different lighting conditions. We analyzed the dynamical features of the model to identify the model mechanisms that produce these responses and investigated the role of light processing dynamics on the responses of the circadian system to light and dark pulses in preschool-aged children.

Methods

The Mathematical Model

In this study, we considered three models of the human circadian pacemaker (Forger et al., 1999; Kronauer et al., 1999; St Hilaire et al., 2007). We show results for all three models in response to napping and non-napping light schedules, however, we focus primarily on the human circadian clock model proposed by Forger et al. because it is the simplest model that produces phase differences consistent with observational data in napping and non-napping preschool children. Therefore, we refer the reader to published detailed descriptions of the other models and briefly summarize the details of the model proposed by Forger and colleagues (Forger et al., 1999). The three-dimensional, deterministic model is defined by the following equations:

$$\frac{dx}{dt} = \frac{\pi}{12}(x_c + B)$$

$$\frac{dx_c}{dt} = \frac{\pi}{12}\left[\mu\left(x_c - \frac{4}{3}x_c^3\right) - x\left[\left(\frac{24}{0.99669\tau_x}\right)^2 + kB\right]\right]$$

$Process\ L$:

$$\frac{dn}{dt} = 60[\alpha(I)(1-n) - \beta n]$$

$$\alpha(I) = \alpha_0\left(\frac{I}{I_0}\right)^p$$

$$B = \hat{B}(1 - 0.4x)(1 - 0.4x_c)$$

$$\hat{B} = G(1-n)\alpha(I)$$

The variable x represents endogenous circadian body temperature, and the variable x_c is a complementary variable. Consistent with the form of the van der Pol oscillator, interactions between x and x_c generate self-sustained, periodic oscillations. The timing of the minimum of x corresponds to the timing of minimum core body temperature (CBT_{min}), a common marker of circadian phase. Alternative definitions of CBT_{min} for the Kronauer model (Kronauer et al., 1999) have been proposed (May et al., 2002); however, to maintain consistency, we defined CBT_{min} as the minimum of the variable x for the three models we considered. The model has been scaled such that the limit cycle solution has an amplitude of 1 and a period of $\tau_x = 24.2$ h in constant darkness.

The third dimension of the model is introduced in Process L, the effect of light exposure on the circadian pacemaker. Process L assumes photoreceptors can be in either an activated or deactivated state with the proportion of activated photoreceptors, n, determined by light intensity, I. The change in state of photoreceptors is determined by the $\frac{dn}{dt}$ equation, and this change is also light-dependent: light entering the system signals the deactivated cells to become activated at a light intensity-dependent and timing-dependent rate, $\alpha(I(t))$. When the light intensity is reduced, the photoreceptors become deactivated at a constant rate, β, independent of $I(t)$.

Process L accounts for both the differential effects of light due to different intensities of light exposure, as well as the timing of light exposure with respect to circadian phase. These effects of light are incorporated through the final two equations, B and $\hat{B}$. The $\hat{B}$ equation represents an intensity-dependent increase in the effect of light and includes the modulation of the light input measured in lux by the activation of photoreceptors. This input is further processed in equation B, which accounts for the circadian phase at which the light signal is received and reflects the phase-dependence of light effects. The model has been fit to and validated on experimental data collected from healthy adults, resulting in the following published parameter values: $\alpha_0 = 0.05\frac{1}{min}, \beta = 0.0075\frac{1}{min}$, $G = 33.75\ min,\ p = 0.5,\ k = 0.55,\ I_0 = 9500\ lux,\ \mu = 0.23$, and $\tau_x = 24.2\ h$ (Forger et al., 1999; Kronauer et al., 1999; Kronauer et al., 2000). All simulations in this study were performed using these validated parameter values.

The model equations were simulated in MATLAB (Mathworks, Natick, MA) and solved numerically using the built-in MATLAB solver **ode45** with relative error tolerance of 1e-9 and an absolute error tolerance of 1e-10. Phase shifts were computed based on the minima of x, which were determined using the built-in MATLAB Signal Processing Toolbox function **findpeaks**.

Simulating Napping vs. Non-napping Light Schedules

We simulated napping and non-napping patterns of light exposure based on published physiological and behavioral data from 20 healthy children (34.2±2.0 months; 11 females; 18 Caucasian, 1 African-American, 1 mixed-race) following their habitual sleep patterns, either habitually napping or non-napping (15 nappers, 5 non-nappers) (Akacem et al., 2015). Napping children had a biphasic sleep pattern and fell asleep during their nap opportunity at least one of the five days (mean +/- SD of napping days: 3.6±1.2) preceding an in-home dim light melatonin onset (DLMO) assessment, the marker used to determine circadian phase. In simulations of the human circadian pacemaker, we entrained the model to fixed light schedules and assessed circadian phase using the minimum of the x variable.

Simulated napping and non-napping patterns of light exposure were developed based on mean sleep timing data reported by Akacem and colleagues (Akacem et al., 2015) (**Figure 1A**). Mean morning wake time was similar for both napping and non-napping children (7:00), but mean bedtime varied between groups; bedtime occurred approximately 45 min earlier in the non-napping (19:33) than in the napping children (20:20). For both groups, the waking light intensity was set to 2241 lux and sleeping light intensity was set to 0 lux based on reported average light levels of preschool-aged children (Hartstein et al., 2022a). However, given the variability of light exposure (Bajaj et al., 2011), we additionally considered the effect of waking light intensity on our findings by simulating patterns with various levels of light intensity during wake (100, 200, 1000, 5000 lux). We also simulated napping and non-napping patterns with reduced light in the evening (setting the light to 200 lux the hour before bedtime to represent a lower indoor light level) to represent more realistic patterns of light exposure. Akacem and colleagues reported the mean nap duration to be 102.6 min centered around 14:43. This mean nap timing and duration was captured in the simulated napping light schedule by setting the light to a dim (2 lux) level for 102 min starting at 13:54 to account for an afternoon nap lighting environment. The low light level for the nap reflects the light intensities reaching the retina through the closed eyelid during the nap when the child is placed in a dim room for a nap opportunity

(Beirman et al., 2011). We assume a dim lighting environment because, although light to the retina is reduced when eyes are closed, there is evidence that sufficient light intensities can penetrate through the eyelids and cause circadian phase shifting (Figueiro and Rea, 2012). We calculated the phase difference between the oscillators for the napping and non-napping groups by first entraining the model to the respective light patterns. To entrain the model, we simulated the model under each (napping and non-napping) light pattern for a minimum of 38 days, at which point the daily CBT_{min} prediction was consistent. We consider these to be the entrained solutions to the periodic forcing of the light patterns. We additionally simulated the model under a typical light pattern for adults: 16:8 light:dark cycle with lights on (2241 lux) beginning at 7:00 and lights off (0 lux) beginning at 11:00 in order to compare the effect of the light schedules on the model response.

Using the built-in MATLAB function **findpeaks**, we determined the timing of the minimum of x for each light pattern simulation. The phase difference is calculated as the difference between the time of the minimum of the non-napping group and the time of the minimum of the napping group. Thus, negative or positive phase shifts indicate that the entrained phase associated with the napping light pattern was delayed or advanced, respectively, when compared to the entrained phase associated with the non-napping light pattern.

In addition to simulating the light patterns previously described, we simulated the nap and bedtime characteristics of the napping pattern of light exposure (Akacem et al.,

2015) independently by creating a nap only pattern (i.e., a nap with an earlier bedtime, 19:33) and a late bedtime only pattern (i.e., no nap with a later bedtime, 20:20). We also varied the conditions of the simulated nap (timing, duration, and light intensity) to determine the contributions of these nap features on the resulting phase difference between models entrained to napping and non-napping light patterns. The start time of the nap was varied between 10:00 and 17:00 to simulate regular morning, afternoon, and evening naps. The nap duration was varied between 0.25 h and 2.5 h. The light level during the nap was varied between 0 and 100 lux to simulate light reaching the retina through a closed eyelid in a dimly lit environment or to simulate a dim napping environment even if the child does not sleep. Baseline conditions for nap start time (13:54), nap duration (1.75 h), and nap light intensity (2 lux) were chosen to be consistent with values in the napping light pattern described above. These features of the nap were varied pairwise and the phase difference from the non-napping light pattern was calculated.

Simulating Phase Response Curves to Light and Darkness

In order to characterize the model's response to stimuli of light or darkness, we adapted a published experimental protocol to determine the PRC to 1 h of bright light and developed an analogous protocol to determine the PRC to 1 h of darkness (St Hilaire et al., 2012). To produce a PRC to light that is representative of the circadian oscillator of a preschool-aged participant on a regular (non-napping) schedule, we utilize the entrained solution to the non-napping light pattern to determine initial conditions for model simulations. In contrast with the experimental PRC protocol, it was not necessary to control for the timing of sleep opportunities in the simulated PRC protocol because the model does not account for sleep homeostasis. Therefore, we eliminated the sleep opportunities and used 29-52 h episodes of dim light to represent the constant routines of varying duration that were specified to distribute light exposure across the 24-h day. Thus, to generate the 1 h PRC to light, the model is initialized with the entrained initial conditions and immediately enters a dim light environment of 2 lux for a variable amount of time (29-52 h). Following this period of constant dim light, the model is then exposed to 1 h of bright light (5000 lux or 150 lux). Then, the model enters a dim light environment for a variable amount of time representing the second constant routine. During the constant dim light periods before and after the light pulse, the timing of the minimum of x, x_{min}, is determined. The phase shift is calculated as the difference between the x_{min} time before and x_{min} time after the light exposure. Thus, negative differences indicate phase delays and positive differences indicate phase advances.

To theoretically understand how the circadian clock would shift due to a pulse of darkness, we simulate an analogous protocol to the one described above and produce theoretical 1 h PRCs to darkness. Using the same entrained initial conditions, the model immediately enters a constant light environment (5000 lux or 150 lux) for a variable amount of time (29-52 h). Next, the model is exposed to 1 h of dim light (2 lux) representing the dark pulse. Following the dark pulse, the model re-enters the original constant light environment. During the constant light periods, the timing of x_{min} is determined both before and after the dark pulse. The phase shift for the PRC to darkness is calculated as described for the PRC to light.

The extended periods of constant background light or constant background darkness in the PRC protocols may produce phase shifting in the model, but the magnitude of the shift will vary with light intensity because the intrinsic period of the oscillator depends on the level of light input (Forger et al., 1999). Thus, to account for phase shifting due to the background light condition, we simulated the model under constant light intensities of 2, 150, and 5000 lux and computed the resulting phase shifts. We then adjusted the PRCs by subtracting the shifts computed under constant conditions from the shifts computed in the presence of the light or dark pulse, according to which light intensity was present in the background constant conditions.

The Model in Constant Conditions and with Perturbations

Given sufficient time and constant light input, $\frac{dn}{dt}$ will reach a steady state value, n_∞, that depends on light intensity. This steady state can be calculated for any light intensity I by setting $\frac{dn}{dt}$ equal to zero and solving for n:

$$\frac{dn}{dt} = 0 = 60[\alpha(I)(1-n) - \beta n]$$

$$n_\infty(I) = \frac{\alpha(I)}{\beta + \alpha(I)}$$

When the model is entrained to a constant light input, the solution trajectory is a self-sustaining limit cycle in a plane specified by $n_\infty(I)$. To study transient solution dynamics, we first entrain the model to a constant light input. Then, we change the light input for 1 h and induce a transient excursion before reverting to the initial light level. We analyze these solutions as one-dimensional time traces, in two-dimensional phase planes, and in the three-dimensional phase space. The velocity along these solution trajectories can be determined by calculating the instantaneous magnitude of the vector field:

$$|\vec{v}| = \sqrt{\left(\frac{dx}{dt}\right)^2 + \left(\frac{dx_c}{dt}\right)^2 + \left(\frac{dn}{dt}\right)^2}$$

Note that under constant light exposure, $\frac{dn}{dt}$ will be 0, so the velocities along limit cycles depend on $\frac{dx}{dt}$ and $\frac{dx_c}{dt}$ only.

Reduction to 2-Dimensional Model

To understand the dynamic contributions of Process L, the light processing component of the model, we considered a reduced version of the model that eliminates the n-dynamics by setting $n = n_\infty(I)$. Thus, the model becomes

$$\frac{dx}{dt} = \frac{\pi}{12}(x_c + B)$$

$$\frac{dx_c}{dt} = \frac{\pi}{12}\left[\mu\left(x_c - \frac{4}{3}x_c^3\right) - x\left[\left(\frac{24}{0.99669\tau_x}\right)^2 + kB\right]\right]$$

$Process\ L$:

$$n = n_\infty(I) = \frac{\alpha(I)}{\beta + \alpha(I)}$$

$$\alpha(I) = \alpha_0\left(\frac{I}{I_0}\right)^p$$

$$B = \hat{B}(1 - 0.4x)(1 - 0.4x_c)$$

$$\hat{B} = G(1 - n)\alpha(I)$$

In the reduced model case, the value of n changes instantaneously with changes in the light input. Using the reduced model, we simulated the previously described napping and non-napping schedules, the adapted light and dark pulse PRC protocols, and simulations with transient solutions due to perturbations. This allows for analysis and comparison of the solution dynamics and the predicted phase shifts between the full and reduced model.

Results

Napping & Non-napping Light Schedules

In these models of the circadian pacemaker, the timing of the minimum of x can be interpreted as the timing of core body temperature minimum (CBT_{min}), an experimental marker of circadian phase. Thus, the phase difference between model simulations under the napping and non-napping light schedules can be calculated based on the predicted timing of CBT_{min} associated with each light pattern. In addition to the childhood light patterns, we simulated an average adult sleep schedule and found that CBT_{min} was predicted to occur at 4:19. With the Forger et al. model, CBT_{min} is predicted to occur at approximately 1:59 and at approximately 2:40 under the non-napping and napping light schedules, respectively. Thus, the predicted phase difference for oscillators on the two different light schedules is approximately 41 min, with the napping schedule delayed in comparison to the non-napping schedule (**Figure 1B**). We find similar results using other mathematical models (**Supplemental Figure 1**) and light intensities (**Supplemental Figure 2**), but the Forger model with the two-intensity (lux) light schedule is the simplest model that is consistent with the observational data. Therefore, we focused on this model for the remainder of our analyses.

Using the model of Forger and colleagues (Forger et al., 1999), we simulated the properties of the napping light pattern independently to understand the distinct contributions of dim light exposure during a nap opportunity and bright light exposure before bedtime. We created a nap only schedule and the late bedtime only schedule as described previously in the methods. Simulating the nap only schedule, CBT_{min} occurs at approximately 2:08; simulating the late bedtime only schedule, CBT_{min} occurs at approximately 2:30 (**Figure 2A**). Thus, when compared with the non-napping schedule, phase delays are predicted for both the nap only schedule (9 min) and the late bedtime only schedule (32 min). These delays collectively produce the 41 min delay predicted with the originally described napping schedule, which includes both the nap and the late bedtime (**Figure 2B**).

Additionally, we varied nap timing, duration, and light intensity to determine how these properties affected phase shifting. When the timing and duration of the nap were allowed to vary, the predicted phase differences between a schedule with a nap and the previously described non-napping light schedule ranged from [0.0137, -0.8352] h (**Figure 2C**). The majority of the naps considered produced phase delays, and the largest delays occurred with naps of the longest duration and earliest timing. The smallest delays and small advances occurred with naps of the longest duration and latest timing. Over the range of low light intensities that we considered, light intensity during the nap minimally impacted predicted phase differences (**Supplementary Figure 3**).

PRC to Light and Darkness

The simulated PRC to light shows both phase and intensity dependence, with the highest sensitivity at the phases around DLMO and the higher light intensity producing larger phase shifts (**Figure 3A**). Similarly, the simulated PRC to darkness also predicts a phase and intensity dependence with the highest sensitivity around DLMO and the higher constant background light level associated with larger shifts (**Figure 3A**). The magnitudes of the phase shifts for the light pulse protocol are larger compared to the magnitudes of the phase shifts for the dark pulse protocol. Additionally, the timing of the minimum phase shift associated with the light pulse occurs slightly earlier compared with the maximum associated with the dark pulse. Given that the intrinsic period of the model varies with the background light level (24.15, 24.01, and 23.9 h for constant 2, 150, and 5000 lux, respectively), the phase shift under constant conditions also varies with light level. Under constant 2, 150, and 5000 lux conditions, we calculated -0.305, -0.049, and 0.165 h shifts, respectively. These values were subtracted from the original PRC predictions to create adjusted PRCs (**Figure 3B**). The asymmetry and phase dependence persist for both the light and the dark pulse adjusted PRCs, however, the intensity dependence is reduced for the adjusted dark pulse PRC compared to the unadjusted dark pulse PRC (**Figure 3B**). The magnitudes of the adjusted phase shifts for the light pulse protocol are larger as compared with the magnitudes of the adjusted phase shifts for the dark pulse protocol in both the 150 lux case ([0.00643, 0.22751] h for the PRC to light and [0.00060, 0.15045] h for the PRC to darkness) (t-test, p=0.00015) and the 5000 lux case ([0.01575, 0.78374] h for the PRC to light and [0.00993, 0.19312] h for the PRC to dark) (t-test, p=2.31e-11).

Model Dynamics in Phase Space

Under constant light conditions, n attains a steady state value that increases asymptotically towards 1 as light intensity increases (**Figure 4A**). Given sufficient time in constant light conditions, the solution trajectory will approach a limit cycle on the $x - x_c$ plane specified by the steady state value of n associated with the constant light input (**Figure 4C**). Limit cycles associated with higher light intensities have smaller amplitudes and shorter intrinsic periods than limit cycles associated with lower light intensities. Thus, solution trajectories associated with a range of constant light inputs form a conic surface when they are plotted in phase space; we approximate this cone with representative light intensities between 0 and 5000 lux (**Figure 4B**). The conic surface is centered at $x = 0$ and shifts towards $x_c = -1$ as n increases (**Figure 4C**). The distance between planes associated with successive values of n also decreases as n approaches 1, reflecting the asymptotic behavior of n_∞ (**Figure 4B**). Additionally, the intrinsic period, and thus the velocity of movement around the limit cycles, depends on n_∞. On planes associated with higher values of n, the velocity along the solution trajectory is smaller compared to the movement on planes associated with lower values of n (**Figure 4D**). For the light intensities we considered, the range of velocity magnitudes is [0.1416, 0.2816]. We also observe that magnitudes vary with the $x - x_c$

location, reflecting the phase dependence in velocities around the limit cycles that is seen explicitly in the B and $\hat{B}$ equations (**Figure 4C**) (Kronauer et al., 1999).

In light schedules with variable light input, such as the napping and non-napping schedules described, solution trajectories move between planes of n (**Figure 1C**). In the non-napping schedule, the trajectory moves between the planes specified by values of n corresponding to the waking light level ($n_\infty(2241\ lux) = 0.76$) and the sleeping light level ($n_\infty(0\ lux) = 0$). For the napping schedule, a third value of n, corresponding to the napping light level, specifies an additional plane ($n_\infty(2\ lux) = 0.09$) that the trajectory approaches. However, in the napping schedule, the nap duration is not long enough for the trajectory to reach the plane specified by $n_\infty(2\ lux)$. Instead, the trajectory approaches this plane during the nap and, at the end of the nap, increased light causes the trajectory to return to the plane specified by $n_\infty(2241\ lux)$. We study the movement of the trajectory between planes specified by different values of n_∞ by analyzing the velocity of n when the starting value of n is varied between $n_\infty(0\ lux) = 0$ and $n_\infty(5000\ lux) = 0.83$, and the new level of light is varied between 0 and 5000 lux. When the light intensity changes, the dynamics of n depend upon both the current value of n and the new light intensity entering the system (**Figure 5B**). The velocity range observed here is [-0.3735, 2.1764], and $\frac{dn}{dt}$ is fastest when beginning at a low light level and receiving a very bright light input. Conversely, $\frac{dn}{dt}$ is slowest when beginning at a high light level and receiving a very dim or dark input.

The asymmetry in the magnitude of predicted phase shifts between the dark pulse and the light pulse protocols resulted from interactions between the differences in the limit cycles associated with the light intensities of the constant conditions and the pulse, as well as the speed at which the trajectory approaches the limit cycle associated with the pulse. To illustrate this, we analyze transient solution trajectories under four different light intensity transitions: decreasing from 150 to 2 lux, decreasing from 5000 to 2 lux, increasing from 2 to 150 lux, and increasing from 2 to 5000 lux (**Figure 5A**). In the dark pulse case, the transient solution moves a smaller distance from the constant light limit cycle as compared with the light pulse case in which the transient solution moves away from the dim light limit cycle (**Figure 5C**). Both the magnitude of the deviation from the limit cycle and the instantaneous magnitude of the vector field, which ranges from [0.1433, 2.1764], are largest when beginning at a low light level and receiving a very bright light input (**Figure 5D**).

Reduced Model Dynamics

To determine the contributions of Process L on the model's predicted phase shifts, we remove the n dynamics and compare the results to the original model. By letting $n = n_\infty$, we reduced the model to a two-dimensional form where changes in light input instantaneously change the value of n. For the specific napping and non-napping patterns of light exposure prescribed by the data (Akacem et al., 2015), similar phase differences were observed in the reduced 2D and full 3D model (39 min and 41 min, respectively). However, both the napping and non-napping schedules predicted CBT_{min} timing that was approximately 25 min later in the reduced model compared to the full model. The PRCs generated with the reduced model showed both phase- and intensity-dependence of light and dark pulses (**Figure 6A**). Phase shifts of similar magnitudes were predicted for both the light pulse and dark pulse protocols with the reduced model, contrasting the asymmetry between the light and dark pulse PRCs generated with the full model. Additionally, by contrast with the results for the 3D model, the PRC for the reduced model showed a greater intensity-dependence for the dark pulse compared to the light pulse. The intrinsic period varied with the background light level (24.15, 24.05, and 23.9 h for constant 2, 150, and 5000 lux, respectively) and, thus, the PRCs were adjusted using the same method as described for the 3D PRCs (**Figure 6B**). Under constant 2, 150, and 5000 lux conditions, the phase shifts were calculated to be -0.334, -0.047, and 0.124 h, respectively. Unlike the adjusted PRCs for the 3D model, the adjusted PRCs for the reduced model continued to exhibit strong phase- and intensity-dependence. In the 150 lux case, the magnitudes of the predicted phase shifts were not significantly different between the light pulse ([0.00062, 0.14119] h) and the dark pulse ([0.00074, 0.15632] h) (t-test, p=0.118). However, asymmetry in the adjusted light and dark pulse PRCs was present in the 5000 lux case with predicted phase shifts that were smaller for the light pulse protocol ([0.00329, 0.26555] h) as compared with the dark pulse protocol ([0.01066, 0.42567] h) (t-test, p=0.00066).

Observing the solution trajectories of the 2D and 3D models in phase space reveals key differences between model solution trajectories that underlie the observed differences in the PRCs associated with these models. In the reduced model, the variable n changes instantaneously to the steady state value associated with each light level. Thus, changes in light levels induce instantaneous jumps between planes associated with different values of n (**Figure 6C**). Comparing the 2D and 3D model PRC predictions, we find that phase dependence is preserved but the magnitudes of the phase shift predictions differ. In the 2D model, the solution trajectory is influenced by only two vector fields: the one associated with the background light level and the one associated with the pulse light level. By contrast, the 3D model solution trajectory travels through continuous planes of n, and each plane's unique vector field influences the movement of the solution trajectory.

Discussion

Using a validated mathematical model of the human circadian oscillator, we determined that differences in patterns of light exposure associated with napping and non-napping light schedules could produce the circadian phase delay observed in napping compared to non-napping preschoolers (Akacem et al., 2015). Simulations of distinct light schedules revealed that both the nap and the later bedtime associated with the napping light schedule contributed to the 41 min predicted phase delay of nappers compared to non-nappers. However, the additional light exposure associated with the later bedtime produced a larger delay than the additional dark exposure associated with the nap. Our results are consistent with previous experimental and modeling work demonstrating that circadian timing is sensitive to different photoperiods (Glickman et al., 2012; Bordyugov et al., 2015; Schmal et al., 2015; Diekman and Bose, 2018; Diekman and Bose, 2022), including our finding that the model under a typical adult light pattern predicted a later circadian phase distinct from both the toddler napping and non-napping patterns.

We also found that the magnitude of phase delays produced by the nap varied with the timing and duration of the nap, with the greatest phase delays occurring for naps with the earliest timings and longest durations. Analysis of model dynamics in phase space provided insight into the dynamical features of the model that produced these observations, as well as the reasons for asymmetry in the effects of light and dark pulses.

Constant light conditions produced limit cycles in the $x - x_c$ plane, forming a cone in the $x - x_c - n$ phase space with the n-dimension of each limit cycle determined by light intensity. At higher light intensities, the amplitude and intrinsic period of the associated limit cycle decrease due to the specified form of the model equations. This feature of the model reflects Aschoff's rule that under increased light intensity, the period of the human circadian pacemaker will decrease (Aschoff, 1960; Kronauer et al., 1999). In addition, dynamics also varied with phase on each limit cycle. By observing transient solution trajectories in the phase space, we found that the slow inactivation rate of photoreceptors in response to a dark pulse results in a small perturbation and a shorter distance for transient solution to travel to return to the bright light limit cycle when the dark pulse ends. By contrast, the fast activation rate of photoreceptors in response to a light pulse leads to a larger perturbation and a longer distance for the transient solution to travel to return to the dim light limit cycle when the light pulse ends. This asymmetry in n dynamics translates to smaller predicted phase shifts with a dark pulse compared with a light pulse, as observed in the simulated dark and light pulse PRCs. By reducing the model to two-dimensions, we made the light effects instantaneous and further highlighted the contribution of n dynamics to this asymmetry. In the reduced 2D model, the magnitude of phase shifting due to light was reduced while the magnitude of phase shifting due to darkness was increased compared to the full 3D model. These findings suggest that the dynamics of light processing play a key role in the properties of the circadian clock model.

Physiology of light processing

Early research on the mammalian eye and its role in circadian regulation indicated that rods and cones were the primary photoreceptors responsible for the communication of light input to the non-visual system (Rodieck, 1998). However, in subsequent years, evidence began to emerge that uncharacterized photoreceptors existed in the eye and were also contributing to the regulation of the non-visual system (Freedman et al., 1999; Lucas et al., 1999; Thapan et al., 2001). This led to the discovery of intrinsically photosensitive retinal ganglion cells (ipRGCs) (Berson et al., 2002). These cells contain melanopsin, a visual pigment, and play a significant role in mediating light exposure's contribution to circadian regulation (Hattar et al., 2002). Furthermore, ipRGCs in mice have been categorized into five types, referred to as M1-M5 (Viney et al., 2007) with each type exhibiting differences in their properties, such as intrinsic photosensitivity and firing rate, and their functions, such as circadian photoentrainment and detecting motion (Ecker et al., 2010; Hu et al., 2013; Zhao et al., 2014). New uncharacterized cell types in the retina are still being discovered (Quattrochi et al., 2019; Young et al., 2021), and the influence of the wavelength of light may be unique for different types of photoreceptors (Berson et al., 2002; Lall et al., 2010; Lucas et al., 2014).

In this study, we were interested in the physiology of light processing during early childhood development. There is a growing literature indicating high circadian sensitivity to light in young children (Higuchi et al., 2014; Akacem et al., 2018; Hartstein et al., 2022a; Hartstein et al., 2022b), and it is thought that this high level of sensitivity may be attributed to physiological changes that occur across the lifespan. Higuchi and colleagues found that, under both dim and bright light conditions, children exhibited larger pupil sizes as compared to their parents (Higuchi et al., 2014). They have also found a correlation in adults between larger pupil diameter and greater melatonin suppression due to light exposure (Higuchi et al., 2008). In addition to changes in pupil size, the clarity of ocular lenses decreases with age. Ocular lenses become increasingly yellow across the lifespan, decreasing the transmission of light to photosensitive cells in the retina (Charman, 2003). Rodent studies have suggested developmentally mediated changes in the light processing communication pathway. Between young and mature mice, the amount of ipRGCs in the retina decreases (Sekaran et al., 2005). As young mice develop, rods and cones begin contributing light information (Schmidt et al., 2008) and there is an increase in the strength of the signals sent to the SCN (Brooks and Canal, 2013). Understanding the developmental changes in the human light processing system will continue to be an important area of research to understand more about the circadian system in early childhood.

Mathematical models of light processing

The mathematical model we focused on in this study includes a phenomenological representation of light processing that was developed based on the idea that a photoreceptor exposed to light will send a signal to the SCN, but in doing so the photopigment within the cell will be unable to send another signal until sufficient time has passed (Kronauer et al., 1999). The model was fit to experimental studies where participants were exposed to very bright light (~9,500 lux) (Khalsa et al., 1997; Forger et al., 1999). There is limited data describing the dynamics of light processing in young children. Later mathematical models of the human circadian clock have refined the light processing dynamics and introduced the effects of non-photic inputs, such as changing sleep-wake status, on the circadian clock (St Hilaire et al., 2007). In this study, we obtained similar results using the Forger et al. model and the model developed by St. Hilaire and colleagues to compare the effects of napping and non-napping light schedules. However, interestingly, the updated light processing proposed by St. Hilaire and colleagues had the greatest effect on light signals below 150 lux. This difference would have a minimal effect under our light protocols since the waking light intensity in our simulations was much higher than 150 lux being set at 2241 lux. However, recent experimental work suggests that the circadian system of young children is highly sensitive to lower light intensities, indicating that the original model of Process L may be better suited to describing the effect of light on the circadian pacemaker of young children. More research is needed to investigate this hypothesis. More recently, other mathematical models have investigated the interactions among different types of ipRGCs (Walch et al., 2015) and considered the effects of different wavelengths of light on phase shifting properties of circadian clock models (Tekieh et al., 2020). Future work extending these findings may establish a physiological basis for the light processing dynamics incorporated In the original model of Process L (Kronauer et al., 1999) .

Predicted phase shifting effects of naps

This simulation-based study suggests that the loss of light exposure associated with a short (1-2 h) nap or nap opportunity in dim light can delay the circadian clock and affect the processing of subsequent light exposure. The cumulative delay effect of a nap and later bedtime may be stronger in young children than adults due to differences in circadian timing and phase of entrainment to sleep onset (LeBourgeois et al., 2013). A previous experimental study in adults found that morning naps advance and evening naps delay circadian phase; afternoon naps, however, did not affect circadian phase (Buxton et al., 2000). The naps in the study by Buxton and colleagues had a duration of 6 h, a much longer duration than the naps typically observed in early childhood. We hypothesize that the nap-induced delay observed in our study occurs due to a reduction in phase advancing afternoon light exposure. The delay, however, is confounded for naps that are sufficiently long to include regions of the dark pulse PRC associated with small advances or delays, particularly when interindividual variability is considered (Crosby, 2005; Crowley and Eastman, 2017; Chellappa, 2021). Furthermore, the model predicts that when a nap occurs during the advance region of the light pulse PRC (in the morning and afternoon), the phase delay due to evening light exposure is larger compared to a non-napping light pattern. This larger phase difference occurs because the decreased light level during the nap amplifies the phase delay induced by light exposure in the evening.

Limitations

There are two main limitations of this work. First, this model was fit to and validated on datasets characterizing the healthy adult circadian clock. At this time, similar datasets characterizing the circadian clock in preschool children are not available. It is therefore unknown how the circadian waveform and response to light differ in early childhood compared with adulthood. Additionally, age related physiological changes in the eye, such as yellowing of lenses and decreased pupil size, have been observed and may influence light processing. Furthermore, light sensitivity in this age group has been found to be high around bedtime (Higuchi et al., 2014; Akacem et al., 2016; Akacem et al., 2018; Hartstein et al., 2022a; Hartstein et al., 2022b). Analyses of the phase shifting properties of the circadian clock in grade school children and adolescents have not identified major differences compared to adults (Crowley and Eastman, 2017; Moreno et al., 2022); additional experimental research utilizing innovative protocols are necessary to address these gaps. Second, the behavioral and observational data used in this study are from a small cohort of healthy, good-sleeping participants. Studies on sleep during early childhood in more diverse participant cohorts are needed to investigate the likely effects of distinct light schedules on the circadian clock.

Conclusions and implications

Using an established model of the adult human circadian pacemaker entrained to light schedules consistent with early childhood, we showed that differences in light exposure associated with napping and non-napping light patterns can produce the observed phase difference in the circadian clocks of napping and non-napping toddlers. Future work applying approaches such as entrainment maps may provide additional insight into differences in oscillator properties between oscillators entrained to the napping or non-napping light schedules, respectively (Diekman and Bose, 2018; Diekman and Bose, 2022). Model analysis revealed a key influence of the dynamics of light processing on predicted phase shifts. However, more experimental research is needed to understand how light sensitivity and dynamics may change across development and to elucidate the impacts of such changes on the circadian system (Higuchi et al., 2014; Hartstein et al., 2022a; Hartstein et al., 2022b). Moreover, studies of historical patterns of light exposure have established that light exposure changes over time with changes in cultural norms and the advent of new technologies (Ekirch, 2016). For example, access to screens is pervasive and becoming more prevalent for humans at all stages of development. There is a growing literature about the effects of screen usage and its relationship to human circadian health and development. Research suggests that increased screen time is associated with delayed bedtimes and shorter total sleep time in children and adolescents (Hale and Guan, 2015; LeBourgeois et al., 2017), and in adults, screen usage before bed suppresses melatonin production and reduces next-morning alertness (Chang et al., 2015). In order to promote the healthy consolidation of sleep during early childhood, as well as to increase treatment efficacy of circadian and sleep disorders across the lifespan, improved understanding of the developing circadian system is of great importance.

Acknowledgements

The authors would like to thank the participants and their families for their contributions to this work. This study was supported in part by the National Institutes of Health Grants K01-MH074643, R01-MH086566, R0I-HD087707, T32-HL149646 and the National Science Foundation Grant DMS 1853511.

Declaration of Conflicting Interests

SRS has no financial or personal conflicts to declare. MKL reports receiving travel funds from the Australian Research Council and research support from the National Institutes of Health, beyond the submitted work. CDB reports receiving research support from the National Institutes of Health, the National Science Foundation, LumosTech, and the Juvenile Diabetes Research Foundation, outside the submitted work.

References

Abraham U, Granada AE, Westermark PO, Heine M, Kramer A, and Herzel H (2010) Coupling governs entrainment range of circadian clocks. Molecular Systems Biology 6:438.

Akacem LD, Simpkin CT, Carskadon MA, Wright KP, Jenni OG, Achermann P, and LeBourgeois MK (2015) The Timing of the Circadian Clock and Sleep Differ between Napping and Non-Napping Toddlers. PLOS ONE 10:e0125181.

Akacem LD, Wright KP, and LeBourgeois MK (2016) Bedtime and evening light exposure influence circadian timing in preschool-age children: A field study. Neurobiol Sleep Circadian Rhythms 1:27-31.

Akacem LD, Wright KP, and LeBourgeois MK (2018) Sensitivity of the circadian system to evening bright light in preschool-age children. Physiological Reports 6:e13617.

Aschoff J (1960) Exogenous and Endogenous Components in Circadian Rhythms. Cold Spring Harbor Symposia on Quantitative Biology 25:11-28.

Bajaj A, Rosner B, Lockley SW, and Schernhammer ES (2011) Validation of a light questionnaire with real-life photopic illuminance measurements: the Harvard Light Exposure Assessment questionnaire. Cancer Epidemiol Biomarkers Prev 20:1341-1349.

Beirman A, Figueiro MG, and Rea MS (2011) Measuring and predicting eyelid spectral transmittance. Journal of Biomedical Optics 16(6).

Berson DM, Dunn FA, and Takao M (2002) Phototransduction by retinal ganglion cells that set the circadian clock. Science 295:1070-1073.

Borbély AA (1982) A two process model of sleep regulation. Hum Neurobiol 1:195-204.

Bordyugov G, Abraham U, Granada A, Rose P, Imkeller K, Kramer A, and Herzel H (2015) Tuning the phase of circadian entrainment. J R Soc Interface 12:20150282.

Boulos Z, and Rusak B (1982) Circadian phase response curves for dark pulses in the hamster. Journal of Comparative Physiology ? A 146:411-417.

Brooks E, and Canal MM (2013) Development of circadian rhythms: role of postnatal light environment. Neurosci Biobehav Rev 37:551-560.

Burgess HJ, and Eastman CI (2004) Early versus late bedtimes phase shift the human dim light melatonin rhythm despite a fixed morning lights on time. Neuroscience Letters 356:115-118.

Buxton OM, L'Hermite-Balériaux M, Turek FW, and van Cauter E (2000) Daytime naps in darkness phase shift the human circadian rhythms of melatonin and thyrotropin secretion. Am J Physiol Regul Integr Comp Physiol 278:R373-382.

Chang A-M, Aeschbach D, Duffy JF, and Czeisler CA (2015) Evening use of light-emitting eReaders negatively affects sleep, circadian timing, and next-morning alertness. Proceedings of the National Academy of Sciences 112:1232-1237.

Charman WN (2003) Age, lens transmittance, and the possible effects of light on melatonin suppression. Ophthalmic Physiol Opt 23:181-187.

Chellappa SL (2021) Individual differences in light sensitivity affect sleep and circadian rhythms. Sleep 44.

Coomans CP, Ramkisoensing A, and Meijer JH (2015) The suprachiasmatic nuclei as a seasonal clock. Front Neuroendocrinol 37:29-42.

Crosby B (2005) Racial Differences in Reported Napping and Nocturnal Sleep in 2- to 8-Year-Old Children. PEDIATRICS 115:225-232.

Crowley SJ, and Eastman CI (2017) Human Adolescent Phase Response Curves to Bright White Light. Journal of Biological Rhythms 32:334-344.

Crowley SJ, Van Reen E, LeBourgeois MK, Acebo C, Tarokh L, Seifer R, Barker DH, and Carskadon MA (2014) A longitudinal assessment of sleep timing, circadian phase, and phase angle of entrainment across human adolescence. PLoS One 9:e112199.

Czeisler CA, Duffy JF, Shanahan TL, Brown EN, Mitchell JF, Rimmer DW, Ronda JM, Silva EJ, Allan JS, Emens JS, Dijk DJ, and Kronauer RE (1999) Stability, precision, and near-24-hour period of the human circadian pacemaker. Science 284:2177-2181.

Czeisler CA, Kronauer RE, Allan JS, Duffy JF, Jewett ME, Brown EN, and Ronda JM (1989) Bright light induction of strong (type 0) resetting of the human circadian pacemaker. Science 244:1328-1333.

Czeisler CA, Richardson GS, Zimmerman JC, Moore-Ede MC, and Weitzman ED (1981) Entrainment of human circadian rhythms by light-dark cycles: a reassessment. Photochem Photobiol 34:239-247.

Daan S, Beersma DG, and Borbély AA (1984) Timing of human sleep: recovery process gated by a circadian pacemaker. Am J Physiol 246:R161-183.

Dibner C, Schibler U, and Albrecht U (2010) The Mammalian Circadian Timing System: Organization and Coordination of Central and Peripheral Clocks. Annual Review of Physiology 72:517-549.

Diekman CO, and Bose A (2018) Reentrainment of the circadian pacemaker during jet lag: East-west asymmetry and the effects of north-south travel. J Theor Biol 437:261-285.

Diekman CO, and Bose A (2022) Beyond the limits of circadian entrainment: Non-24-h sleep-wake disorder, shift work, and social jet lag. J Theor Biol 545:111148.

Duffy JF, and Wright KP (2005) Entrainment of the Human Circadian System by Light. Journal of Biological Rhythms 20:326-338.

Duffy JF, Zitting K-M, and Chinoy ED (2015) Aging and Circadian Rhythms. Sleep Medicine Clinics 10:423-434.

Dumont M, and Beaulieu C (2007) Light exposure in the natural environment: relevance to mood and sleep disorders. Sleep Med 8:557-565.

Dunlap JC (1999) Molecular bases for circadian clocks. Cell 96:271-290.

Dwyer SM, and Rosenwasser AM (2000) Effects of light intensity and restraint on dark-pulse-induced circadian phase shifting during subjective night in Syrian hamsters. J Biol Rhythms 15:491-500.

Ecker JL, Dumitrescu ON, Wong KY, Alam NM, Chen S-K, Legates T, Renna JM, Prusky GT, Berson DM, and Hattar S (2010) Melanopsin-Expressing Retinal Ganglion-Cell Photoreceptors: Cellular Diversity and Role in Pattern Vision. Neuron 67:49-60.

Ekirch AR (2016) Segmented Sleep in Preindustrial Societies. Sleep 39:715-716.

Figueiro MG, and Rea MS (2012) Preliminary evidence that light through the eyelids can suppress melatonin and phase shift dim light melatonin onset. BMC Res Notes 5:221.

Forger DB, Jewett ME, and Kronauer RE (1999) A Simpler Model of the Human Circadian Pacemaker. Journal of Biological Rhythms 14:533-538.

Forger DB, and Peskin CS (2003) A detailed predictive model of the mammalian circadian clock. Proc Natl Acad Sci U S A 100:14806-14811.

Foster RG, Provencio I, Hudson D, Fiske S, De Grip W, and Menaker M (1991) Circadian photoreception in the retinally degenerate mouse (rd/rd). Journal of Comparative Physiology A 169:39-50.

Freedman MS, Lucas RJ, Soni B, von Schantz M, Muñoz M, David-Gray Z, and Foster R (1999) Regulation of mammalian circadian behavior by non-rod, non-cone, ocular photoreceptors. Science 284:502-504.

Gachon F, Nagoshi E, Brown SA, Ripperger J, and Schibler U (2004) The mammalian circadian timing system: from gene expression to physiology. Chromosoma 113:103-112.

Gleit RD, Diniz Behn CG, and Booth V (2013) Modeling Interindividual Differences in Spontaneous Internal Desynchrony Patterns. Journal of Biological Rhythms 28:339-355.

Glickman G, Webb IC, Elliott JA, Baltazar RM, Reale ME, Lehman MN, and Gorman MR (2012) Photic Sensitivity for Circadian Response to Light Varies with Photoperiod. Journal of Biological Rhythms 27:308-318.

Hale L, and Guan S (2015) Screen time and sleep among school-aged children and adolescents: A systematic literature review. Sleep Medicine Reviews 21:50-58.

Hannay KM, Booth V, and Forger DB (2019) Macroscopic Models for Human Circadian Rhythms. Journal of Biological Rhythms 34:658-671.

Hannay KM, Forger DB, and Booth V (2018) Macroscopic models for networks of coupled biological oscillators. Sci Adv 4:e1701047.

Hardin PE, Hall JC, and Rosbash M (1990) Feedback of the Drosophila period gene product on circadian cycling of its messenger RNA levels. Nature 343:536-540.

Hartstein LE, Behn CD, Akacem LD, Stack N, Wright KP, and LeBourgeois MK (2022a) High sensitivity of melatonin suppression response to evening light in preschool-aged children. J Pineal Res 72:e12780.

Hartstein LE, Diniz Behn C, Wright KP, Akacem LD, Stowe SR, and LeBourgeois MK (2022b) Evening Light Intensity and Phase Delay of the Circadian Clock in Early Childhood. J Biol Rhythms:7487304221134330.

Hattar S, Liao HW, Takao M, Berson DM, and Yau KW (2002) Melanopsin-containing retinal ganglion cells: architecture, projections, and intrinsic photosensitivity. Science 295:1065-1070.

Higuchi S, Ishibashi K, Aritake S, Enomoto M, Hida A, Tamura M, Kozaki T, Motohashi Y, and Mishima K (2008) Inter-individual difference in pupil size correlates to suppression of melatonin by exposure to light. Neurosci Lett 440:23-26.

Higuchi S, Nagafuchi Y, Lee S-I, and Harada T (2014) Influence of Light at Night on Melatonin Suppression in Children. The Journal of Clinical Endocrinology & Metabolism 99:3298-3303.

Honma K-i, and Honma S (1988) A Human Phase Response Curve for Bright Light Pulses. The Japanese Journal of Psychiatry and Neurology 42:167-168.

Hu C, Hill DD, and Wong KY (2013) Intrinsic physiological properties of the five types of mouse ganglion-cell photoreceptors. J Neurophysiol 109:1876-1889.

Iglowstein I, Jenni OG, Molinari L, and Largo RH (2003) Sleep duration from infancy to adolescence: reference values and generational trends. Pediatrics 111:302-307.

Jenni OG, and LeBourgeois MK (2006) Understanding sleep–wake behavior and sleep disorders in children: the value of a model. Current Opinion in Psychiatry 19:282-287.

Jewett ME, Kronauer RE, and Czeisler CA (1991) Light-induced suppression of endogenous circadian amplitude in humans. Nature 350:59-62.

Jewett ME, Kronauer RE, and Czeisler CA (1994) Phase-Amplitude Resetting of the Human Circadian Pacemaker via Bright Light: A Further Analysis. Journal of Biological Rhythms 9:295-314.

Kennaway DJ, Goble FC, and Stamp GE (1996) Factors influencing the development of melatonin rhythmicity in humans. J Clin Endocrinol Metab 81:1525-1532.

Kennaway DJ, Stamp GE, and Goble FC (1992) Development of melatonin production in infants and the impact of prematurity. J Clin Endocrinol Metab 75:367-369.

Khalsa SBS, Jewett ME, Cajochen C, and Czeisler CA (2003) A Phase Response Curve to Single Bright Light Pulses in Human Subjects. The Journal of Physiology 549:945-952.

Khalsa SBS, Jewett ME, Klerman EB, Duffy JF, Rimmer DW, Kronauer RE, and Czeisler CA (1997) Type 0 Resetting of the Human Circadian Pacemaker to Consecutive Bright Light Pulses Against A Background of Very Dim Light. Sleep Research 26:722.

Kim JK, and Forger DB (2012) A mechanism for robust circadian timekeeping via stoichiometric balance. Molecular Systems Biology 8:630.

Kronauer RE, Czeisler CA, Pilato SF, Moore-Ede MC, and Weitzman ED (1982) Mathematical model of the human circadian system with two interacting oscillators. Am J Physiol 242:R3-17.

Kronauer RE, Forger DB, and Jewett ME (1999) Quantifying Human Circadian Pacemaker Response to Brief, Extended, and Repeated Light Stimuli over the Phototopic Range. Journal of Biological Rhythms 14(6):501-516.

Kronauer RE, Forger DB, and Jewett ME (2000) Errata: Quantifying Human Circadian Pacemaker Response to Brief, Extended, and Repeated Light Stimuli over the Photopic Range. Journal of Biological Rhythms 15:184-186.

Lall GS, Revell VL, Momiji H, Al Enezi J, Altimus CM, Güler AD, Aguilar C, Cameron MA, Allender S, Hankins MW, and Lucas RJ (2010) Distinct contributions of rod, cone, and melanopsin photoreceptors to encoding irradiance. Neuron 66:417-428.

LeBourgeois MK, Carskadon MA, Akacem LD, Simpkin CT, Wright KP, Achermann P, and Jenni OG (2013) Circadian phase and its relationship to nighttime sleep in toddlers. J Biol Rhythms 28:322-331.

LeBourgeois MK, Hale L, Chang A-M, Akacem LD, Montgomery-Downs HE, and Buxton OM (2017) Digital Media and Sleep in Childhood and Adolescence. Pediatrics 140:S92-S96.

Lucas RJ, Freedman MS, Muñoz M, Garcia-Fernández JM, and Foster RG (1999) Regulation of the mammalian pineal by non-rod, non-cone, ocular photoreceptors. Science 284:505-507.

Lucas RJ, Peirson SN, Berson DM, Brown TM, Cooper HM, Czeisler CA, Figueiro MG, Gamlin PD, Lockley SW, O'Hagan JB, Price LL, Provencio I, Skene DJ, and Brainard GC (2014) Measuring and using light in the melanopsin age. Trends Neurosci 37:1-9.

May CD, Dean DA, and Jewett ME (2002) A revised definition of core body temperature phase that incorporates both state variables of a limit-cycle human circadian pacemaker model improves model stability at low circadian amplitudes. In, pp 22-26, Society for Research on Biological Rhythms Annual Meeting.

Meijer JH, Michel S, and Vansteensel MJ (2007) Processing of daily and seasonal light information in the mammalian circadian clock. Gen Comp Endocrinol 152:159-164.

Minors DS, Waterhouse JM, and Wirz-Justice A (1991) A human phase-response curve to light. Neurosci Lett 133:36-40.

Mirsky HP, Liu AC, Welsh DK, Kay SA, and Doyle FJ (2009) A model of the cell-autonomous mammalian circadian clock. Proc Natl Acad Sci U S A 106:11107-11112.

Mohawk JA, Green CB, and Takahashi JS (2012) Central and Peripheral Circadian Clocks in Mammals. Annual Review of Neuroscience 35:445-462.

Moore RY, and Eichler VB (1972) Loss of a circadian adrenal corticosterone rhythm following suprachiasmatic lesions in the rat. Brain Res 42:201-206.

Moore RY, Speh JC, and Card JP (1995) The retinohypothalamic tract originates from a distinct subset of retinal ganglion cells. J Comp Neurol 352:351-366.

Moreno JP, Hannay KM, Walch O, Dadabhoy H, Christian J, Puyau M, El-Mubasher A, Bacha F, Grant SR, Park RJ, and Cheng P (2022) Estimating circadian phase in elementary school children: leveraging advances in physiologically informed models of circadian entrainment and wearable devices. Sleep 45.

Oster H (2006) The genetic basis of circadian behavior. Genes Brain Behav 5 Suppl 2:73-79.

Piltz SH, Diniz Behn CG, and Booth V (2020) Habitual sleep duration affects recovery from acute sleep deprivation: A modeling study. J Theor Biol 504:110401.

Price JL, Blau J, Rothenfluh A, Abodeely M, Kloss B, and Young MW (1998) double-time is a novel Drosophila clock gene that regulates PERIOD protein accumulation. Cell 94:83-95.

Provencio I, Rodriguez IR, Jiang G, Hayes WP, Moreira EF, and Rollag MD (2000) A Novel Human Opsin in the Inner Retina. The Journal of Neuroscience 20:600-605.

Quattrochi LE, Stabio ME, Kim I, Ilardi MC, Michelle Fogerson P, Leyrer ML, and Berson DM (2019) The M6 cell: A small-field bistratified photosensitive retinal ganglion cell. Journal of Comparative Neurology 527:297-311.

Ralph MR, Foster RG, Davis FC, and Menaker M (1990) Transplanted suprachiasmatic nucleus determines circadian period. Science 247:975-978.

Rodieck RW (1998) The first steps in seeing. Sinauer Associates, Sunderland, MA.

Roenneberg T, and Foster RG (1997) Twilight times: light and the circadian system. Photochem Photobiol 66:549-561.

Rosenwasser AM, and Dwyer SM (2002) Phase shifting the hamster circadian clock by 15-minute dark pulses. J Biol Rhythms 17:238-247.

Schmal C, Myung J, Herzel H, and Bordyugov G (2015) A theoretical study on seasonality. Front Neurol 6:94.

Schmidt TM, Taniguchi K, and Kofuji P (2008) Intrinsic and extrinsic light responses in melanopsin-expressing ganglion cells during mouse development. J Neurophysiol 100:371-384.

Sekaran S, Lupi D, Jones SL, Sheely CJ, Hattar S, Yau KW, Lucas RJ, Foster RG, and Hankins MW (2005) Melanopsin-dependent photoreception provides earliest light detection in the mammalian retina. Curr Biol 15:1099-1107.

Skeldon AC, Derks G, and Dijk DJ (2016) Modelling changes in sleep timing and duration across the lifespan: Changes in circadian rhythmicity or sleep homeostasis? Sleep Med Rev 28:96-107.

St Hilaire MA, Gooley JJ, Khalsa SBS, Kronauer RE, Czeisler CA, and Lockley SW (2012) Human phase response curve to a 1 h pulse of bright white light. The Journal of Physiology 590:3035-3045.

St Hilaire MA, Klerman EB, Khalsa SB, Wright KP, Czeisler CA, and Kronauer RE (2007) Addition of a non-photic component to a light-based mathematical model of the human circadian pacemaker. J Theor Biol 247:583-599.

Stack N, Zeitzer JM, Czeisler C, and Diniz Behn C (2020) Estimating Representative Group Intrinsic Circadian Period from Illuminance-Response Curve Data. Journal of Biological Rhythms 35:195-206.

Stephan FK, and Zucker I (1972) Circadian Rhythms in Drinking Behavior and Locomotor Activity of Rats Are Eliminated by Hypothalamic Lesions. Proceedings of the National Academy of Sciences 69:1583-1586.

Sumová A, Bendová Z, Sládek M, Kováciková Z, and Illnerová H (2004) Seasonal molecular timekeeping within the rat circadian clock. Physiol Res 53 Suppl 1:S167-176.

Tekieh T, Lockley SW, Robinson PA, McCloskey S, Zobaer MS, and Postnova S (2020) Modeling melanopsin-mediated effects of light on circadian phase, melatonin suppression, and subjective sleepiness. J Pineal Res 69:e12681.

Thapan K, Arendt J, and Skene DJ (2001) An action spectrum for melatonin suppression: evidence for a novel non-rod, non-cone photoreceptor system in humans. The Journal of Physiology 535:261-267.

Turner PL, and Mainster MA (2008) Circadian photoreception: ageing and the eye's important role in systemic health. British Journal of Ophthalmology 92:1439-1444.

Van Cauter E, Sturis J, Byrne MM, Blackman JD, Leproult R, Ofek G, L'Hermite-Balériaux M, Refetoff S, Turek FW, and Van Reeth O (1994) Demonstration of rapid light-induced advances and delays of the human circadian clock using hormonal phase markers. Am J Physiol 266:E953-963.

Viney TJ, Balint K, Hillier D, Siegert S, Boldogkoi Z, Enquist LW, Meister M, Cepko CL, and Roska B (2007) Local retinal circuits of melanopsin-containing ganglion cells identified by transsynaptic viral tracing. Curr Biol 17:981-988.

Walch OJ, Zhang LS, Reifler AN, Dolikian ME, Forger DB, and Wong KY (2015) Characterizing and modeling the intrinsic light response of rat ganglion-cell photoreceptors. J Neurophysiol 114:2955-2966.

Welsh DK, Logothetis DE, Meister M, and Reppert SM (1995) Individual neurons dissociated from rat suprachiasmatic nucleus express independently phased circadian firing rhythms. Neuron 14:697-706.

Welsh DK, Takahashi JS, and Kay SA (2010) Suprachiasmatic nucleus: cell autonomy and network properties. Annu Rev Physiol 72:551-577.

Wright KP, Gronfier C, Duffy JF, and Czeisler CA (2005) Intrinsic Period and Light Intensity Determine the Phase Relationship between Melatonin and Sleep in Humans. Journal of Biological Rhythms 20:168-177.

Yamazaki S, Numano R, Abe M, Hida A, Takahashi R, Ueda M, Block GD, Sakaki Y, Menaker M, and Tei H (2000) Resetting central and peripheral circadian oscillators in transgenic rats. Science 288:682-685.

Young BK, Ramakrishnan C, Ganjawala T, Wang P, Deisseroth K, and Tian N (2021) An uncommon neuronal class conveys visual signals from rods and cones to retinal ganglion cells. Proceedings of the National Academy of Sciences 118:e2104884118.

Zeitzer JM, Dijk DJ, Kronauer RE, Brown EN, and Czeisler CA (2000) Sensitivity of the human circadian pacemaker to nocturnal light: melatonin phase resetting and suppression. The Journal of Physiology 526:695-702.

Zhao X, Stafford BK, Godin AL, King WM, and Wong KY (2014) Photoresponse diversity among the five types of intrinsically photosensitive retinal ganglion cells. The Journal of Physiology 592:1619-1636.

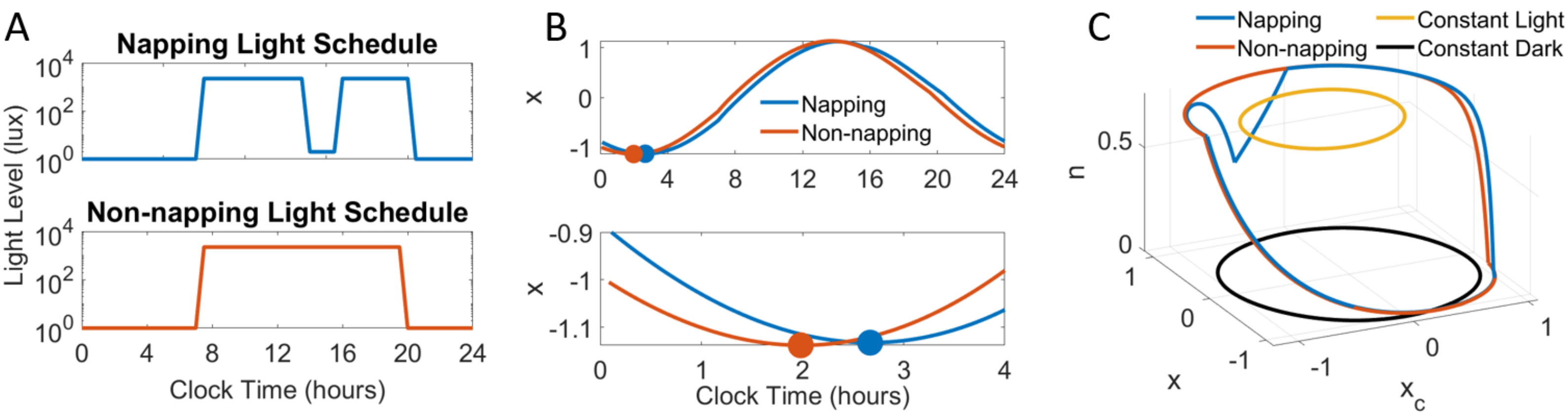

Figure 1: Napping and non-napping light schedules produce distinct solution trajectories and circadian phase predictions. (A) 24-h napping and non-napping light schedules describe light timing and intensities during nighttime sleep, waking, and napping. Waking light intensity is 2241 lux and sleeping light intensity is 0 lux for both schedules. In the napping schedule, the light was set to 2 lux from 13:54 to 15:36 to simulate a 102 min nap centered around 14:45. Wake time is 7:00 in both schedules, and bedtime differed between the two schedules by 43 min (bedtime is 20:20 in the napping schedule, and 19:33 in the non-napping schedule). (B) Simulation time traces of the circadian variable, x, under the napping and non-napping light schedules show that the circadian phase is delayed in the napping schedule compared to the non-napping schedule. The predicted timing of the minimums of x, representing minimum core body temperature, occur at 1:59 for the non-napping schedule and 2:40 for the napping schedule. Thus, the non-napping schedule produces an advance in circadian phase of approximately 41 min compared to the napping schedule. (C) Phase space solution trajectories, including constant light and constant dark limit cycles.

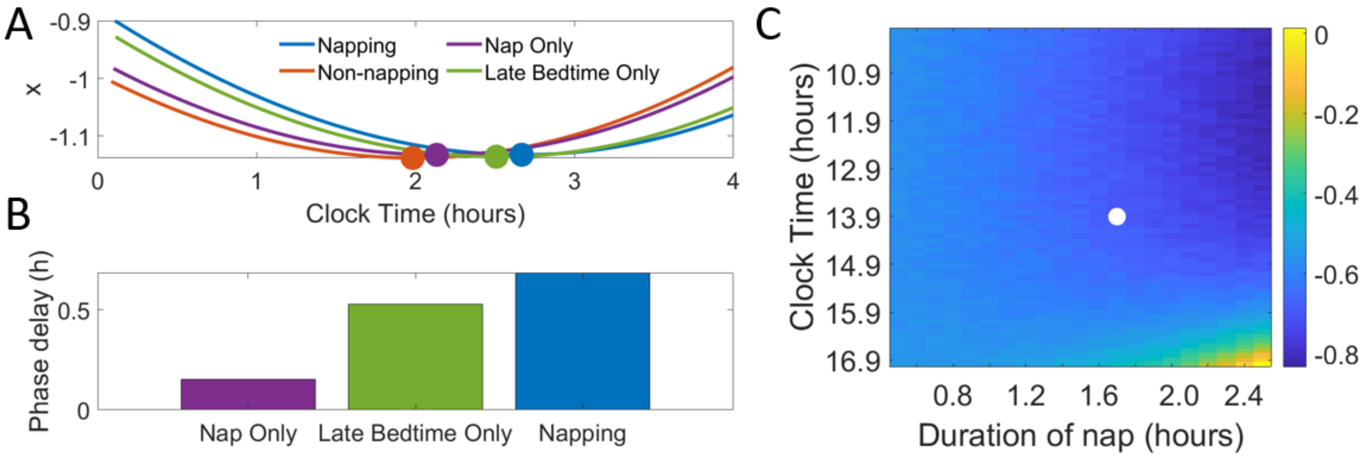

Figure 2: Contributions of nap and bedtime on phase shifts and the effects of varying nap properties. Light intensities for wake, sleep, and nap and the napping and non-napping light schedules are as in Figure 1. (A) Four regular light schedules are simulated: napping (timing and durations as in the napping schedule in Figure 1); nap only (102 min nap occurrence from 13:54 to 15:36 and bedtime at 19:33); late bedtime only (no nap and bedtime set to 20:20); and non-napping (timing and durations as in the non-napping schedule in Figure 1). The four light schedules are associated with four distinct circadian phases between 1:59 and 2:40. (B) The non-napping schedule produces the earliest entrained circadian phase. The nap only, late bedtime only, and napping schedules produce circadian phases that are delayed with respect to the non-napping schedule by 0.15 h, 0.53 h, and 0.69 h respectively. (C) The heat map reports the calculated phase difference between the non-napping schedule and variations of the napping schedule (negative values are phase delays). The largest phase differences occur for long naps that occur early in the day, and the smallest phase differences occur for long naps that occur late in the day. The white marker indicates the nap start time and nap duration associated with the default napping light schedule.

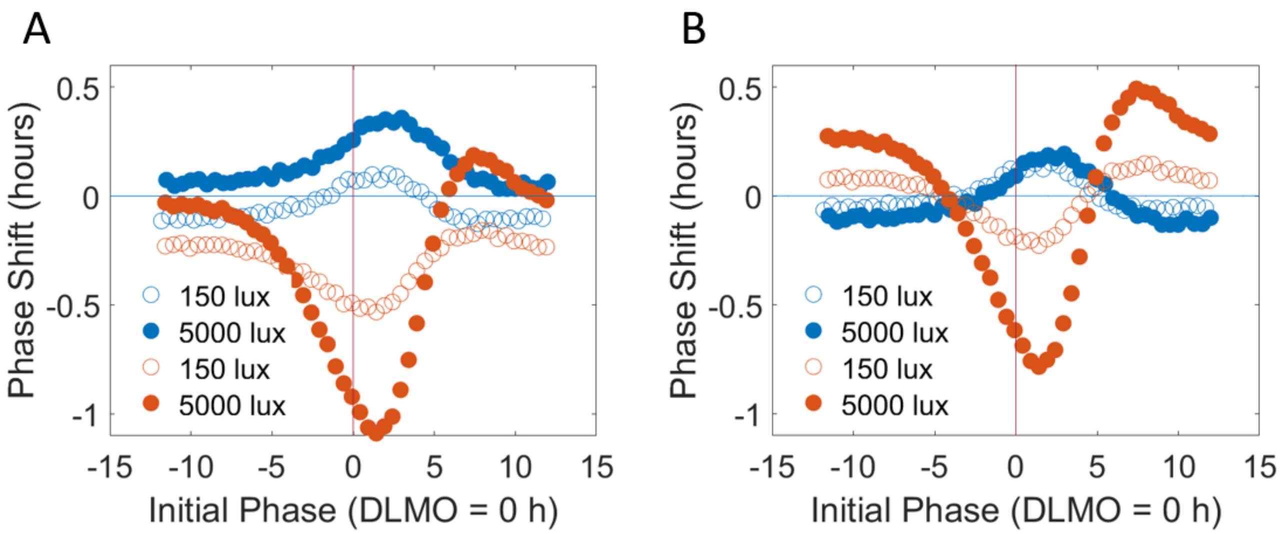

Figure 3: Simulated phase response curves (PRCs) to a 1 h exposure of light or dark. Each PRC protocol was simulated with early childhood initial conditions generated from the non-napping schedule. For the light pulse PRCs, a 1 h light exposure of 150 (open) or 5000 (closed) lux is administered between constant dim periods of 2 lux and produces PRCs with troughs slightly after DLMO = 0 h. For the dark pulse PRCs, a 1 h dark exposure of 2 lux is administered between constant light periods with two background light intensities of 150 (open) or 5000 (closed) lux and produces PRCs with peaks slightly after DLMO = 0 h. (A) PRCs show both intensity dependence and phase dependence for both light and dark stimuli. The light pulses produce larger magnitude phase shifts compared with the dark pulses at most circadian phases. 5000 lux light pulses or background conditions produce larger phase shifts in the light and dark pulse PRCs, respectively. (B) Adjusting the PRCs to account for phase shifting due to constant background light conditions and the system's intrinsic period preserves phase dependence in both the light and dark pulse PRCs but reduces the intensity dependence in the dark pulse PRCs.

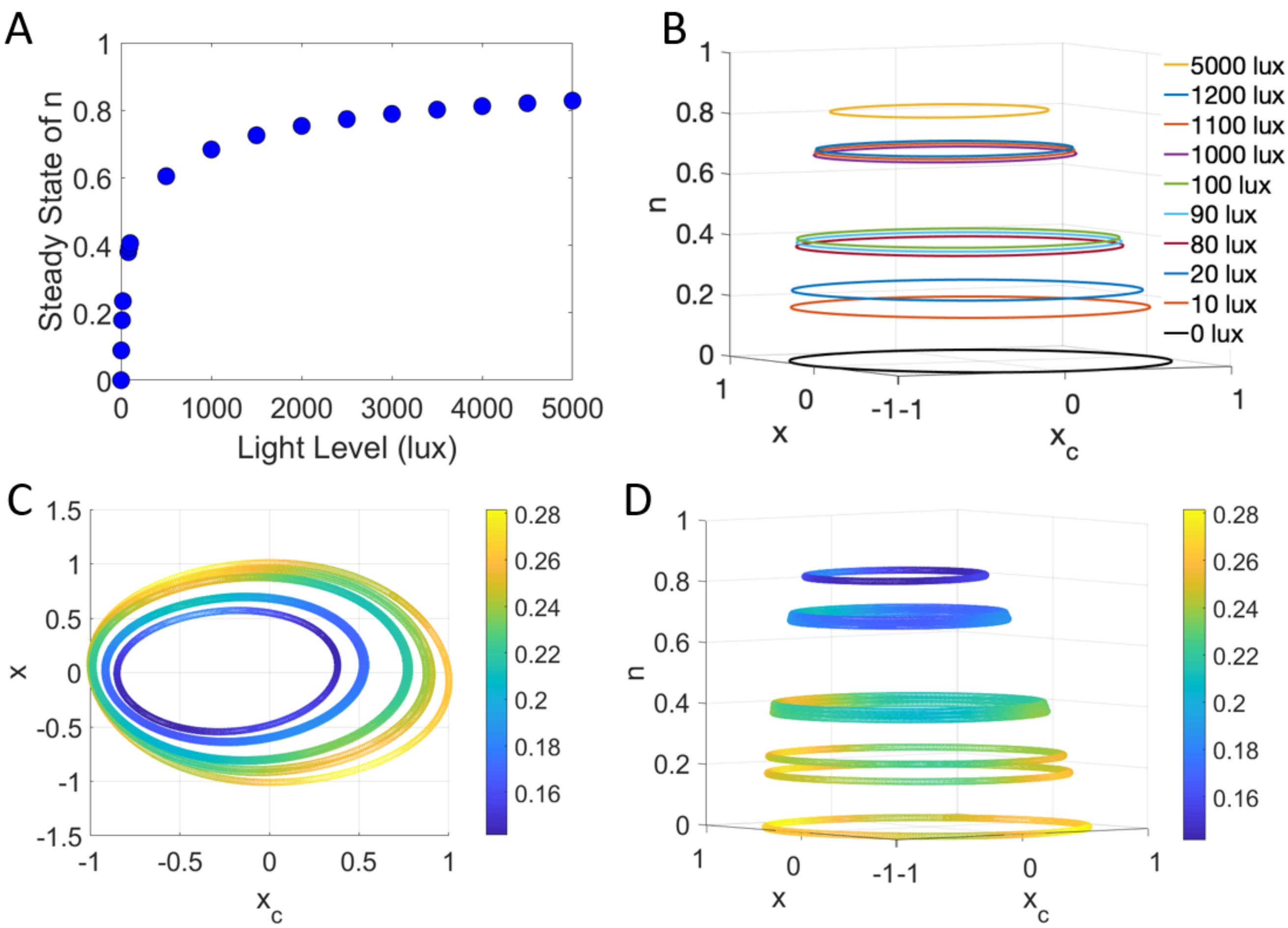

Figure 4: In constant light conditions, the solution trajectories form a cone of asymmetric limit cycles on planes corresponding to the steady state of n. (A) The steady state value of n, n_∞, depends on (constant) light intensity and increases asymptotically towards 1 as the light level increases. (B) Limit cycle solutions for constant light inputs ranging from 0 to 5000 lux in the $x - x_c - n$ phase space. The amplitude of oscillations and the vertical distance between solutions both decrease as constant light intensity increases. (C) Limit cycle solutions projected into the $x - x_c$ plane. The magnitude of the $[dx/dt\, , dx_c/dt]$ vectors, denoted by the color bar, represents velocities around the limit cycles in the $x - x_c$ plane. As indicated by the colors, the velocity of the solution varies with phase around each limit cycle. (D) Velocity of limit cycle solutions for constant light inputs ranging from 0 to 5000 lux in the $x - x_c - n$ phase space varies inversely with n_∞ such that velocities are slower on the limit cycles associated with high light levels compared to the velocities on limit cycles associated with low light levels.

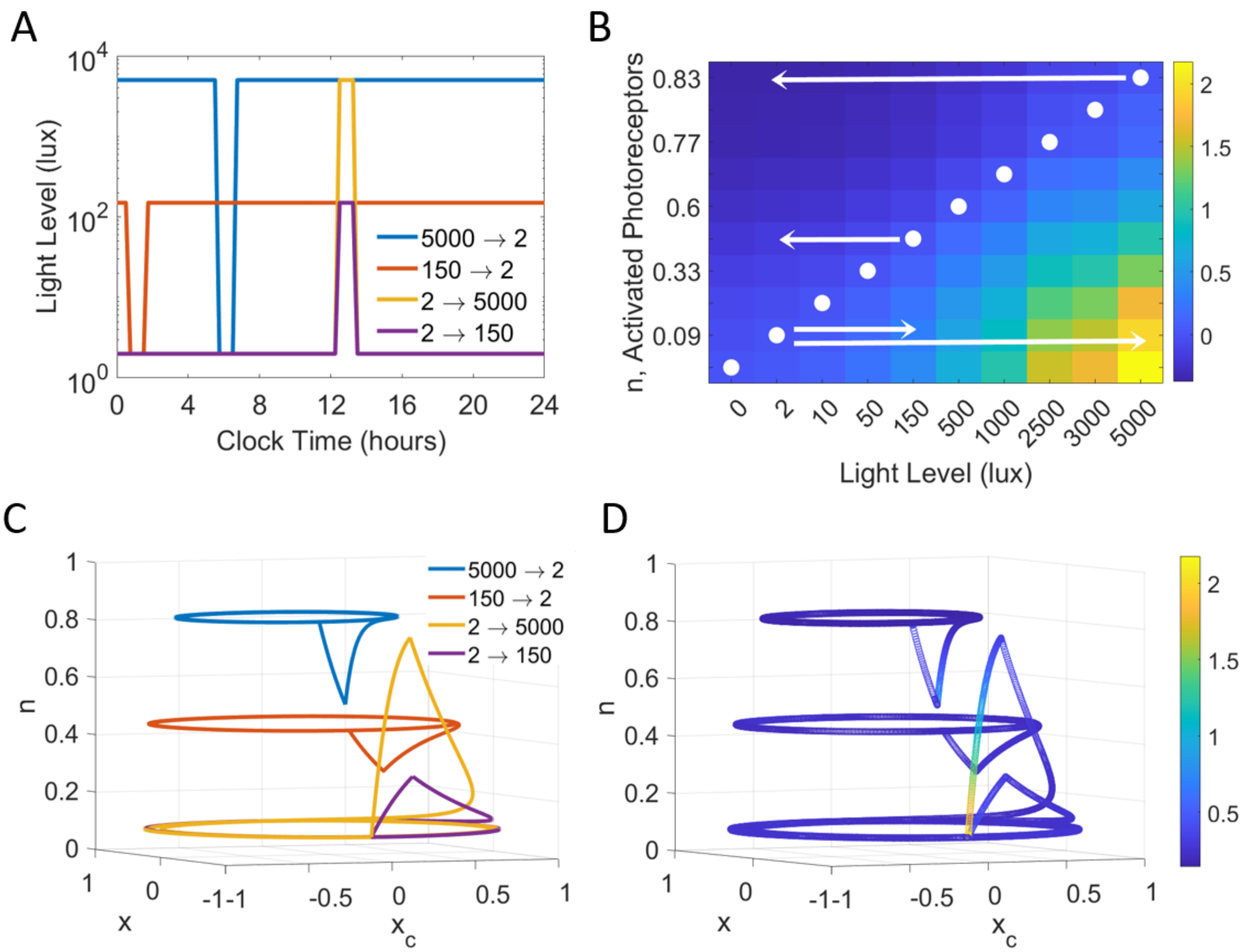

Figure 5: Transient solution dynamics depend on both the starting light level and the magnitude of the change in light intensity. (A) 24-h light schedules for transient solution simulations. Two schedules involve a dark pulse of 2 lux at the time of the minimum of x, with background light set to 150 lux or 5000 lux. Additionally, two schedules involve a light pulse of 150 lux or 5000 lux at the time of the minimum of x, with background light set to 2 lux. (B) The heat map shows how the velocity of n, dn/dt, varies with light level and n value. The fastest changes in n occur when n is low and light intensity is high. The white circles indicate the steady state value of n for each light level. Arrows indicate the transitions in light intensities when light level is decreased from 5000 or 150 lux to 2 lux or increased from 2 lux to 150 or 5000 lux as occurs in the PRC simulations. (C) Four solution trajectories in the $x - x_c - n$ phase space approach limit cycles associated with constant light conditions and show transient excursions away from these limit cycles due to increases or decreases in light intensity. (D) Magnitude of velocity vector $[dx/dt,\ dx_c/dt\ , dn/dt]$ along four solution trajectories in the $x - x_c - n$ phase space that approach limit cycles associated with constant light conditions and show transient excursions away from these limit cycles due to increases or decreases in light intensity.

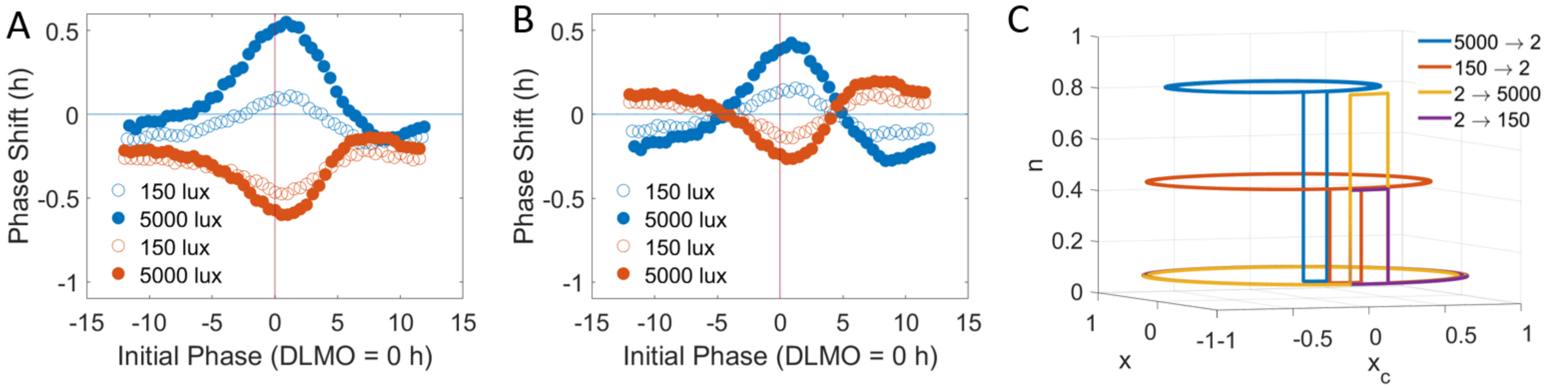

Figure 6: Eliminating n dynamics alters the phase shifting properties of the model. In the 2D model, n dynamics are eliminated by setting $n = n_\infty$. The light and dark pulse PRC protocols described in Figure 3 were simulated for the 2D model with early childhood initial conditions generated from the non-napping schedule. (A) PRCs for the 2D model show both intensity dependence and phase dependence for both light and dark stimuli. In contrast with the 3D model, the dark pulses produce larger magnitude shifts compared with the light pulses at most circadian phases. (B) Adjusting the PRCs for the 2D model to account for phase shifting due to constant background light conditions and the model system's intrinsic period preserves phase dependence in both the light and dark pulse PRCs but reduces the intensity dependence in the dark pulse PRCs. (C) Four solution trajectories for the 2D model plotted in the $x - x_c - n$ phase space show instantaneous changes in n with changes in light intensity. When changes in n are instantaneous, n dynamics do not contribute to the observed phase shifts due to changes in light intensity.

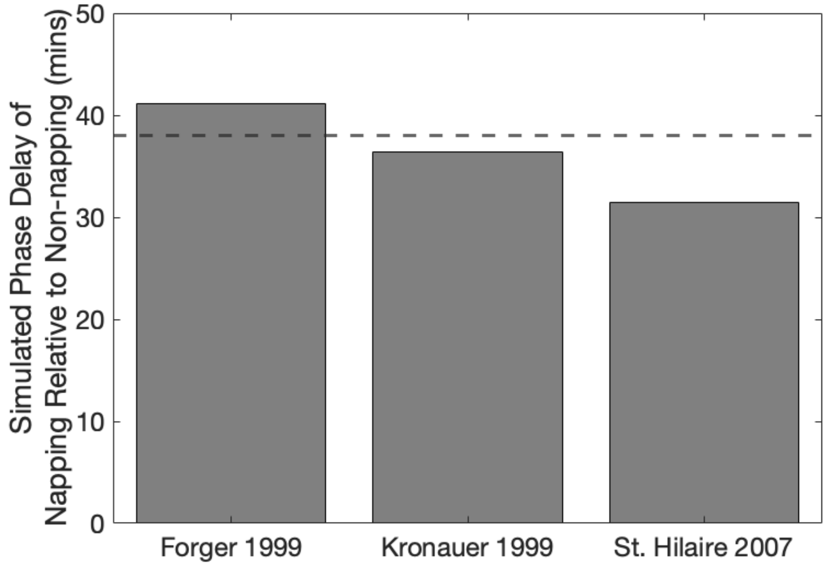

Supplemental Figure 1: Model choice affects the predicted phase difference between the entrained napping and non-napping light schedules. All three models considered predicted the CBT_{min} of the napping schedule to be delayed compared to the non-napping schedule, with schedules as described in Figure 1. The St. Hilaire model (St Hilaire et al., 2007) with non-photic inputs predicts the smallest phase delay of 31 minutes. The Kronauer model (Kronauer et al., 1999) predicts a phase delay of 36 minutes. The Forger model (Forger et al., 1999) predicts a phase delay of 41 minutes. The mean phase delay observed in preschool-aged children is 38 mins (Akacem et al., 2015) denoted by the dashed line.

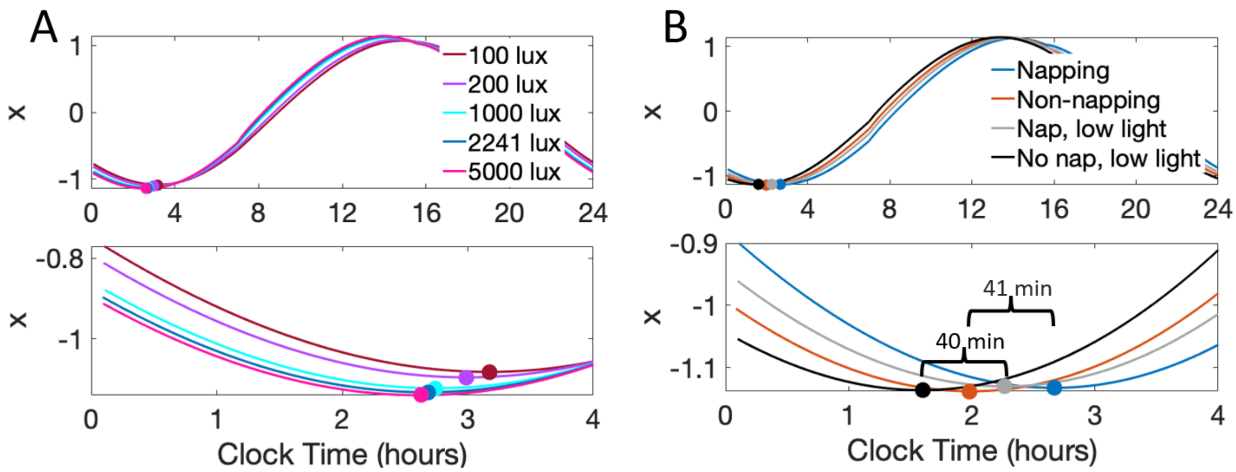

Supplemental Figure 2: Light intensity during wake has minor effects on predicted CBT_{min} timing prediction and decreased light intensity in the evening has minor effects on the phase difference between the napping and non-napping light schedules. (A) Simulation time traces of the circadian variable, x, under the napping light schedule with sleeping light intensity set to 0 lux and napping light intensity set to 2 lux as in Figure 1. The waking light intensity is varied from 100 lux to 5000 lux with predicted CBT_{min} timing varying from 3:10 to 2:37. For lower waking light intensities, the predicted CBT_{min} occurs earlier. (B) More realistic light schedules with lower light intensities before bedtime produce similar differences between napping and non-napping schedules compared to schedules with a single light intensity throughout the waking period. Simulation time traces of the circadian variable, x, under the napping (blue) and non-napping (orange) light schedules as described in Figure 1 show a 41 minute phase difference. Simulation time traces of the circadian variable, x, under the napping schedule (gray) and non-napping schedule (black) with one hour of lower intensity light (200 lux) before bedtime (19:20 – 20:20 and 18:33 – 19:33, respectively) show a 40 minute phase difference.

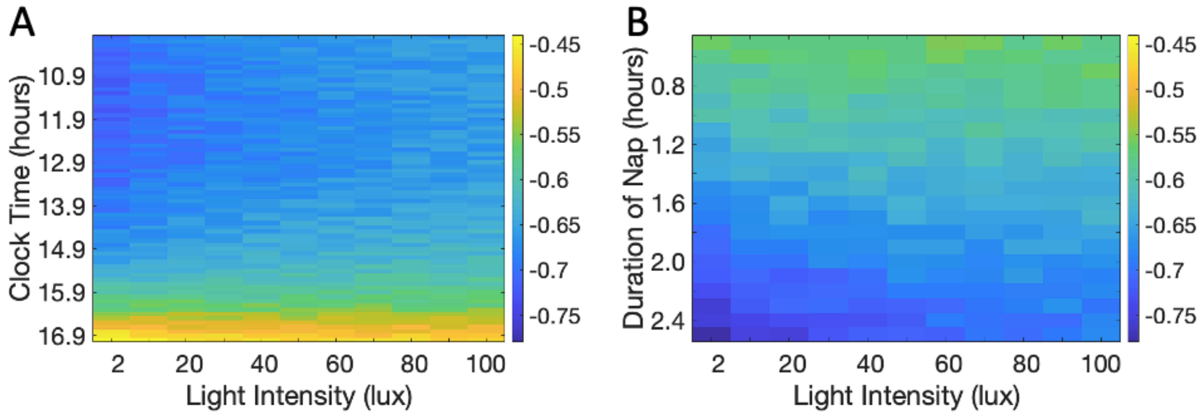

Supplemental Figure 3: Light intensity during the nap has minor effects on predicted phase shifting. Heat maps showing contributions of nap light intensity, start time, and duration on predicted phase shifting. Light levels for wake and sleep, and the non-napping light schedule are as in Figure 1. The heat maps report the calculated phase difference between the non-napping schedule and variations of the napping schedule (negative values are phase delays). Light intensity during the nap varies between [2, 100] lux. All reported combinations of nap features predict the napping schedule to be phase delayed when compared to the non-napping schedule. (A) We varied nap start time between [10:00, 17:00] and fixed nap duration at 102 min. The magnitude of the phase shifts ranged between [-0.7269, -0.4218] h. The largest phase delays occurred for the lowest light intensity and early nap start time. (B) We varied nap duration between [0.5, 2.5] h and fixed nap start time at 13:54. The magnitude of the phase shifts ranged between [-0.7788, -0.5538] h. The largest phase delays occurred with the lowest light intensity and longest nap duration.